Raman and 2D electronic spectroscopies: a fruitful alliance for the investigation of ground and excited state vibrations in chlorophyll *a*

Elena Meneghin†, Danilo Pedron†, Elisabetta Collini*
Department of Chemical Sciences, University of Padova

Keywords

Vibrational and vibronic coherence; 2D electronic spectroscopy; Raman spectroscopy; resonance enhancement.

Abstract

Vibrational coherences and their time evolution are crucial for the correct description of the dynamical behavior of materials, also influencing the dynamics of electronic coherences and transport processes. For this reason, vibrational coherences are now becoming the subject of wider investigation, especially in the framework of 2D electronic spectroscopies. A correct interpretation of vibrational coherences in 2DES responses requires the comparison with Raman spectra.

Here we propose a methodology that goes beyond the typical practice of merely looking for frequencies present in both signals. In particular, we discuss suitable experimental conditions and correction procedures that allows a direct comparison of Fourier spectra obtained from the analysis of the signal beating at specific coordinates in 2D maps with resonant and non-resonant Raman spectra, to clearly identify the vibrational modes more strongly coupled with the electronic transition.

The advantages of this approach have been illustrated using Chl*a* chromophore as a case study.

† These authors contributed equally to this work.

*Corresponding author.

E-mail address: elisabetta.collini@unipd.it

1. Introduction

2D electronic spectroscopy (2DES) techniques are recently gaining increasing interest given their capability of following ultrafast energy transport and relaxation processes in real time. The reason for their success is mainly linked to the possibility of preparing and monitoring coherent states and verify how they contribute to the overall relaxation dynamics of the system.

The evolution of a coherent superposition of states is manifested in the experimental signals as oscillations in the amplitude as a function of time [1,2]. The analysis of this oscillating behavior is a critical point in the interpretation of 2DES responses and the ensuing description of the dynamic behavior of the studied system.

For many years since the development of the 2DES techniques, the attention of the researchers has been mainly focused on the quest of experimental evidence for long-lived *electronic* coherences [3–5], directly correlated to a possible enhancement of the transport performances in light-harvesting complexes. In this context, the unavoidable presence also of vibrational coherences was mainly treated as a disturbance, hindering the more appealing oscillations associated with electronic coherences, and considered to be not entirely relevant for the dynamics of the system.

In more recent publications, instead, vibrational coherences and their time evolution have been recognized as crucial for a correct description of the dynamical behavior of the materials, also influencing the dynamics of electronic coherences [6–8]. For this reason, vibrational [9] and vibronic [10] coherences, previously disdained, are now becoming the subject of broader investigation, especially in the framework of 2DES spectroscopies.

The possibility to exploit the ultrafast oscillatory evolution of a third-order signal to extract information about normal modes [11–14] and their coupling with electronic transitions [15] has been known for some time, but the increased dimensionality of 2DES techniques allows a novel insight into such a well-studied topic.

Along with this line, we have recently demonstrated the crucial role of the coupling between excited electronic states and a specific manifold of vibrational modes in the relaxation dynamics of chlorophyll a (Chl*a*). Chl*a* is the most abundant photoactive chromophore in Nature, being the primary pigment responsible for photosynthetic function in green plants [16–18]. Given the importance of this dye, the electronic and vibrational properties of Chl*a* has been intensively studied since the 60's through several time- and frequency-resolved techniques. [19–29] More recently, Chl*a* has also been the object of an intense investigation through 2DES spectroscopy in different conditions [30–33]. In these works, a lot of attention has been paid in identifying how the coupling with the environment and with vibrational degrees of freedom can affect the electronic and optical properties of the molecule. The main idea is to investigate which particular nuclei motions are more strongly coupled with the electronic transitions and verify if they have any role in the ensuing relaxation or transport dynamics.

In principle, 2DES is particularly suitable for this task because, according to the prediction of the simple displaced harmonic oscillator (DHO) model, the signatures arising from vibrational coherences occur in distinguishable positions in 2DES map [34,35], and thus their behavior can be analyzed studying the signal at these positions. In practice, the effect of the finite laser bandwidth and broadening, particularly severe at room temperature, often complicates this task and call for the comparison with other experimental data.

Several spectroscopic techniques have been proposed and successfully applied to characterize vibrational modes and their coupling with electronic transitions, the most famous ones being Raman spectroscopy, hole burning, fluorescence line narrowing, and three-pulse photon echo peak shift technique. In particular, Raman spectra are often cited as support for the interpretation of vibrational beatings in 2DES spectra. The Raman response is indeed particularly suitable for the comparison with 2DES spectroscopy. Indeed, it is more convenient than other vibrational spectroscopies for several reasons.

First, like 2DES, Raman is a third order technique. It requires the interaction of the molecular system with three electric fields, whose frequency can be tuned to be far from an electronic transition of the systems (NRR) or resonant with it (RR). The comparison of the intensities of the signals in NRR and RR spectra provides information on the modes more strongly coupled with the resonant electronic transition specifically excited. If the RR spectrum is measured in resonance with the same electronic transition investigated in the 2DES spectroscopy, a direct comparison can be made.

Another significant advantage is the possibility of also investigating low-frequency modes (< 500 cm^{-1}), that often result crucial in the coupling with electronic degrees of freedom, especially in transport processes.

Nowadays database of Raman spectra of the major artificial and biological pigments is available, and the development of user-friendly commercial equipment has made the Raman technique an easily accessible routine method. It is therefore very tempting for the 2DES spectroscopist to merely recover a Raman spectrum and make a direct comparison with the Fourier spectrum of the oscillations found in the 2DES response. While this procedure is absolutely legitimate and it allows for an easy and quick first preliminary identification of vibrational modes in the 2DES maps, much more details and information could be extracted from a more conscious analysis of the spectra.

In this work, 2DES and Raman spectroscopy have been combined to provide a thorough characterization of the vibrational modes more strongly coupled with the lowest energy electronic transition (Q_y-bands).

2. Experimental

2.1 Sample preparation

Chl*a* from spinach was purchased from Sigma Aldrich and used without further purification. 2DES measures have been performed on solutions of Chl*a* in methanol (MeOH) with a concentration of about 50 μM at room temperature. The absence of aggregates has been ascertained verifying that the normalized steady-state absorption spectrum does not show any significant modification lowering the concentration down to two orders of magnitude. Steady-state absorption spectra were acquired before and after each scan to control that no degradation of the sample occurred during the 2DES measurements.

Raman measures could not be performed in MeOH solution because it was not possible to obtain concentrations high enough without aggregation. The RR and NRR Raman spectra have then been performed directly on Chl*a* powders at 77K.

2.2 2DES spectroscopy

2DES measurements have been conducted with the setup described in Ref. [36].
Briefly, the output of a 800 nm, 3 KHz Ti:Sapphire laser system (Coherent Libra) is converted in a broad visible pulse in a non-collinear optical amplifier (Light Conversion TOPAS White). The spectrum has been tuned to cover mainly the Q_y transition to characterize the relaxation dynamics of the lowest excited state as shown in Fig. 1(b).
The transform-limited condition for the pulses at the sample position is achieved through a prism compressor coupled with a Dazzler pulse shaper for the fine adjustment. The pulse duration, optimized through FROG measures [37], is 9 fs (Fig. S1, Appendix A), corresponding to a spectral bandwidth of 1640 cm^{-1}. The pulses energy at the sample position is reduced to 9 nJ per pulse by a broadband half-waveplate/polarizer system.
The 2DES experiment relies on the passively phase stabilized setup, where the laser output is split into four identical phase-stable beams (three exciting beams and a fourth beam further attenuated of 3 orders of magnitude and used as Local Oscillator, LO) in a BOXCARS geometry using a suitably designed 2D grating. Pairs of 4° CaF2 wedges modulate time delays between pulses. One wedge of each pair is mounted onto a translation stage that regulates the thickness of medium crossed by the exciting beam and provides a temporal resolution of 0.07 fs. Delay times t_1 (coherence time between first and second exciting pulses), t_2 (population time between second and third exciting pulses) and t_3 (rephasing time between the third exciting pulses and the emitted signal) are defined.
The outcome of the experiment is a 3D matrix of data describing the evolution of 2D frequency-frequency correlation maps, where the two frequencies ω_1 and ω_3 are obtained Fourier transforming t_1 and t_3, respectively, as a function of t_2. Rephasing and non rephasing spectra were acquired for population times ranging from 0 to 2 ps in 7.5 fs increments, with each experiment repeated three times to ensure reproducibility.
The non-coherent time evolution of the 2DES signal along t_2 is analyzed through recently proposed global fitting procedures [31] and subtracted. To identify the main frequency components contributing to the beating pattern, several methods have been proposed [39]. Here, a Fourier transform of the oscillating residues at selected coordinates has been performed to obtain a so-called Fourier spectrum.

2.3 Raman spectroscopy

Raman spectra have been performed with a home-built micro-Raman system, based on a Triax-320 ISA spectrograph, equipped with a holographic 1800 g/mm grating and a CCD detector (Spectrum One ISA Instruments). The excitation sources were a Spectra Physics Ar^+ laser operating at 514.5 nm and an He-Ne laser at 632.8 nm for non-resonant and resonant conditions, respectively. Appropriate edge filters were used to reduce the stray-light level. An Olympus BX 40 optical microscope equipped with a long working distance 50x/0.50 objective was optically coupled to the spectrograph. The Raman spectra were recorded on Chl*a* powders between 100 and 2000 cm^{-1} and with an instrumental resolution of about 2 cm^{-1}. To avoid optical damage, readily occurring at room temperature, the sample was held in a cryostat cell (Linkam Scientific Instruments) at 77K and the power of the exciting radiation was maintained between 0.2 and 0.4 mW. At this temperature, the frequency and linewidth of the Raman peaks, especially the ones at low frequency, could slightly change with respect to room temperature. However, considering that the peaks in the Fourier spectra

of 2DES oscillating traces are anyhow at least one order of magnitude broader than the peaks in Raman spectra, any possible temperature-dependent change could be readily neglected in the comparison between Raman and 2DES signals reported below.

3. Results

3.1 Preliminary characterization

Fig. 1 reports the molecular structure of Chl*a* (panel (a)). In panel (b) the steady-state absorption and fluorescence spectra of Chl*a* solution in MeOH are reported together with the exciting conditions employed in 2DES and Raman experiments.

The electronic properties of Chl*a* are typically described using the Gouterman's four orbital model [19,20] which predicts two groups of transitions conventionally labelled as B and Q bands, falling at higher and lower energies, respectively. In particular, the Q-bands of Chl*a* spectrum are the result of two (possibly overlapping) independent electronic transitions called Q_x ($S_0 \rightarrow S_2$) and Q_y ($S_0 \rightarrow S_1$), with *x* and *y* indicating the polarization directions within the macrocycle plane, as in Fig. 1(a).

The bands related to those transitions are broadened by inhomogeneous effects and by the activation of low-frequency molecular vibrations. Higher energy vibronic transitions appear instead as separated sidebands, usually identified as $Q_y(0,1)$ and $Q_x(0,1)$, respectively. The lowest energy band at 660 nm (15180 cm^{-1}) is assigned to $Q_y(0,0)$ transition, while higher energies signals are attributed to the mixing of $Q_y(0,n)$ and Q_x states [29,40].

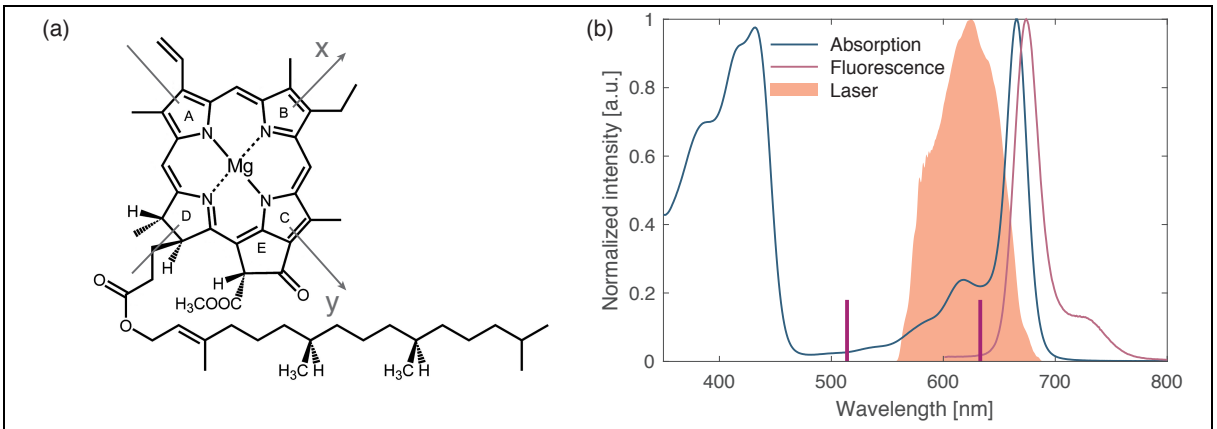

Fig. 1. (a) Molecular structure of Chl*a*. The directions of dipole moments are also reported. (b) Steady-state absorption (blue line) and fluorescence emission spectra (pink line, exc. 600 nm) of Chl*a* solution in MeOH. The orange area represents the experimental exciting laser spectrum used in 2DES spectroscopy, whereas the purple sticks pinpoint the excitation frequency in RR (633 nm) and NRR (514 nm) experiments. The intensities of the spectra are normalized to 1 on their maxima.

3.2 2DES

2DES spectra have been measured tuning the exciting profile on the blue side of the Q_y band. This choice allows exploiting the spectral profile as a sort of spectral filter [41–43] to specifically select contributions of ground (excited) state vibrations in the rephasing (non rephasing) part of the signal, as discussed in detail below.

The obtained results are summarized in Fig. 2. Both rephasing and non rephasing maps (panel (a)) shows the typical features expected for isolated Chl*a* molecules. The main diagonal positive peak at around (15250, 15250) cm^{-1} arises from stimulated emission and ground state bleaching of the $Q_y(0,0)$ band. The cross-peak at about (16500, 15250) cm^{-1} is instead originated by the coupling of the $Q_y(0,0)$ state with vibrational modes within the range 1000-1300 cm^{-1}, responsible also for the vibronic progression in the linear absorption spectrum, and by ultrafast relaxation processes from higher states [33].

Rephasing signal decay along the population time can be described with a bi-exponential function with time constants 140 fs and $\gg$ 2 ps (Fig. 2(b)). The first component is negligible in non rephasing signal that decays with a time constant much longer than the investigated time window. As already discussed in the literature, the ultrafast component is readily associated with the spectral diffusion whereas the second time constant describes all the relaxation phenomena characterized by longer timescales, such as population relaxation, not fully appreciable in our limited time window.

More interesting is the beating behavior of the maps along t_2. Indeed, the analysis of the oscillating part of the signal revealed several beating components, that can be attributed to ground and/or excited state vibrational coherences. We are particularly interested in the vibrational modes more strongly coupled with the electronic transition and therefore more strongly affecting the potential energy curve of the excited state. These are indeed the modes potentially involved in the enhancement of the efficiency of biological functions in Chl*a*-binding photosynthetic proteins [44,45].

The are several simplified models proposed to identify vibronic coherences in the excited state. The starting point common to all approaches is the DHO model where the system is represented by two electronic states, g and e, which are coupled to a vibrational mode with frequency Ω. The vibronic potential energy surface of the e state is shifted up by electronic transition energy ε and its minimum is shifted by d with respect to the ground state g (scheme in Fig. 3(a)). This setup results in two vibrational ladders of quantum sub-states g_m and e_n [46,47].

Starting from this model and applying the semiclassical perturbation theory with respect to the incoming fields, the system-field interaction and evolution sequences, can be revealed. These sequences, often denoted by the Liouville space pathways, can be graphically represented by Feynman diagrams, particularly useful in identifying at which coordinates different evolution pathways contribute to 2DES maps.

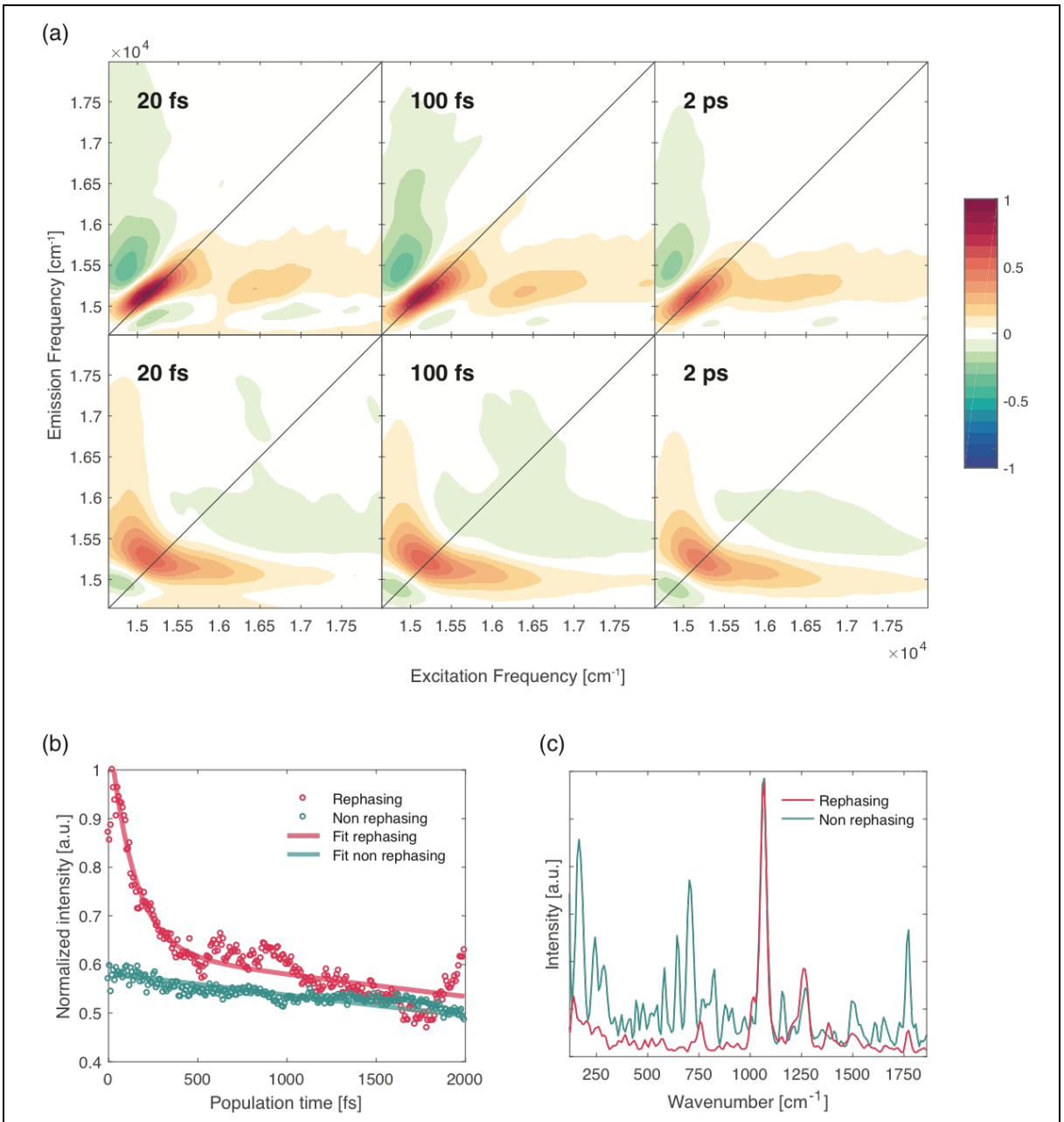

Fig. 2. (a) Evolution of 2DES rephasing (upper row) and non rephasing (lower row) maps of Chl*a* in MeOH at selected values of population time. (b) Rephasing (red) and non rephasing (green) signal decays at coordinates (15180,15180) cm^{-1}. Experimental data (circles) and bi-exponential fittings (lines) resulting from global analysis. (c) Fourier spectra of the residues at coordinates $(\varepsilon, \varepsilon + \Omega)$ of rephasing and non rephasing data.

According to the prediction of the DHO model, the signatures arising from vibrational coherences of the ground and the excited state occurs in distinguishable positions in 2DES map, and thus both their energy and dephasing times can in principle be characterized separately. In particular, the signals arising from vibrational coherences and contributing to the rephasing signal form a characteristic chair-pattern of five contributions [34]. The pattern is reversed in non rephasing spectra, as shown in Fig. 3(b). The cross-peaks at coordinates

$(\varepsilon, \varepsilon \pm \Omega)$, where ε in this specific case is the energy of the $Q_y(0,0)$ electronic transition, are crucial to disentangle and characterize the dynamics of the excited and ground state vibrational coherences since the two contributions are not superimposed at these coordinates [34,35].

Specific 2DES schemes, suitably designed to capture the coherent dynamics at these coordinates [30] and mixed vibrational electronic fifth-order multidimensional techniques [48], have also been proposed.

Here we suggest a more straightforward procedure that does not require any modification of the 2DES setup but that just exploits the comparison between rephasing and non rephasing signal and a careful choice of the exciting spectral bandwidth to be used as spectral filter. Indeed, tuning the spectrum of the exciting pulses toward the blue of the lowest energy $Q_y(0,0)$ transition allows capturing only 3 (4) out of the 5 oscillating signals expected in rephasing (non rephasing) experiment. Moreover, at coordinates $(\varepsilon, \varepsilon + \Omega)$ the oscillating signal is specifically attributable to a vibrational coherence only in the excited or ground state in rephasing and non rephasing spectra, respectively (Fig. 3(b)).

One could argue that it would be possible to obtain the same information exciting directly in the middle of the absorption band so to capture the whole 5-signal patterns and compare the behavior of the beating at coordinates $(\varepsilon, \varepsilon + \Omega)$ and $(\varepsilon, \varepsilon - \Omega)$ in the rephasing signal. While this is certainly true, our choice presents at least two advantages. First, the analyzed peaks fall at the same coordinates in the 2DES maps, and therefore they can be more easily compared without possible artefacts due to the comparison in different spectral regions. Second, the analyzed signals correspond both to anti-Stokes Raman signals (i.e., they appear at a detection frequency higher than the center frequency of the exciting pulses), expected to be more intense in agreement with the results of stimulated Raman scattering experiments [49].

From the careful analysis of the signals occurring in those two positions, the main vibrational coherences of the ground and the excited state were detected and shown in the form of Fourier spectra in Fig. 2(c). The frequencies of all the identified modes are reported in Table S1 (Appendix A).

The main finding emerging from the comparison of the Fourier spectra in Fig. 2(c) is that in the rephasing signal, associated with excited state vibrational coherences, two main bands in the region 1000-1300 cm^{-1}, precisely at 1070 and 1270 cm^{-1}, dominate the beating pattern. In the non rephasing signal, instead, a richer pattern is found with several modes also contributing at lower (< 800 cm^{-1}) and higher (between 1300 and 1700 cm^{-1}) frequency regions.

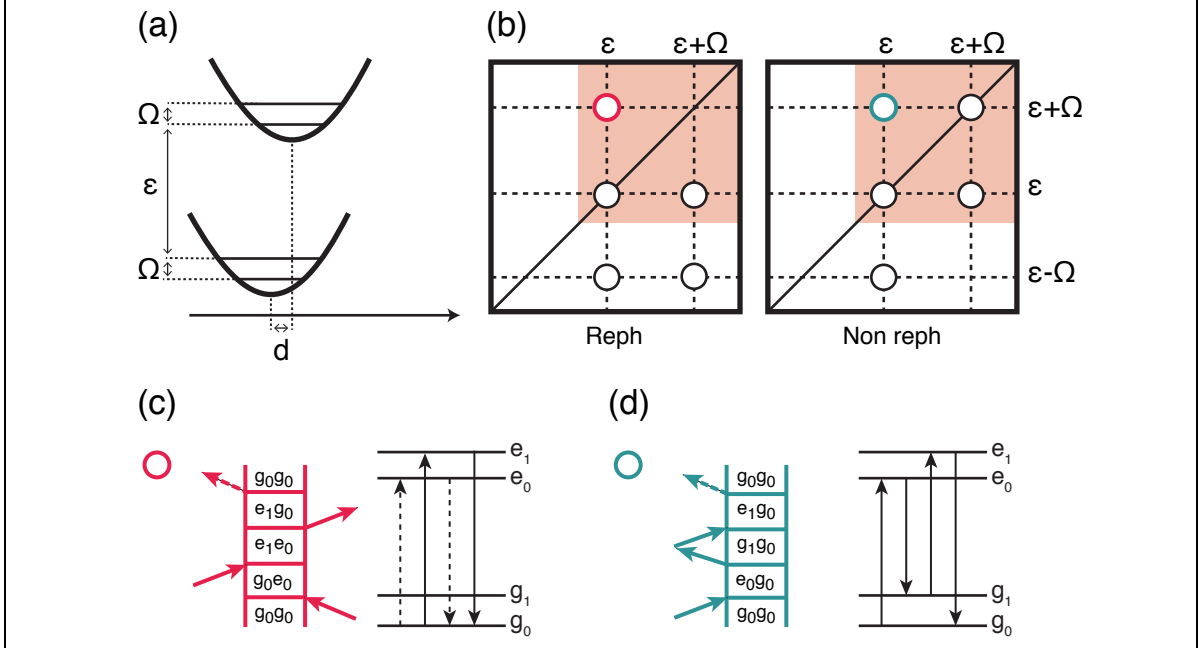

Fig. 3. (a) Displaced oscillator model. (b) Schemes representing the amplitude pattern of a vibrational coherence beating at frequency Ω in rephasing and non rephasing maps. The orange shadowed area represents the spectral filter operated by the pulse bandwidth. A red (green) marker pinpoints the position in rephasing (non rephasing) spectra where only excited (ground) state vibrational coherences contribute. (c) Double sided and ladder diagrams describing the beating contribution at coordinates $(\varepsilon, \varepsilon + \Omega)$ in rephasing spectrum (red). (d) Double sided and ladder diagrams describing the beating contribution at coordinates $(\varepsilon, \varepsilon + \Omega)$ in non rephasing spectrum (green).

3.3 Raman

The Raman spectra have been recorded in non resonant (NRR, exciting at 514 nm) and resonant conditions (RR, exciting at 633 nm). Note that the exciting wavelength in RR spectra matches the central wavelength of the broadband pulse employed in 2DES. We are thus allowed to exploit the comparison of NRR and RR spectra with the 2D data, as support for the identification of modes more strongly coupled to Q_y electronic transition.

However, to achieve a meaningful comparison between RR and NRR, the spectra must be preliminarily suitably corrected to account for the different experimental conditions. Fig. 4 compares the RR and NRR spectra of Chl*a* powders after various steps of correction. Native Raman spectra recorded in the two exciting conditions are reported in Fig. 4(a).

The first crucial step consists in correcting the Raman spectra for the different response of the molecular system in different spectral regions and under different exciting conditions. Fluorescence is a significant challenge in Raman spectroscopic analysis of organic and biological specimens because, if fluorescence is generated, it is often much more intense than Raman scattering and it can hide Raman features [50].

It is clear that the relative intensity between fluorescence and Raman signal strongly depends on the excitation wavelength, with the fluorescence background getting stronger in resonant conditions. Usually, if the fluorescence signal is not completely hiding the Raman scattering, as in Chl*a* case, it is possible to remove this contribution subtracting the fluorescence profile from the background.

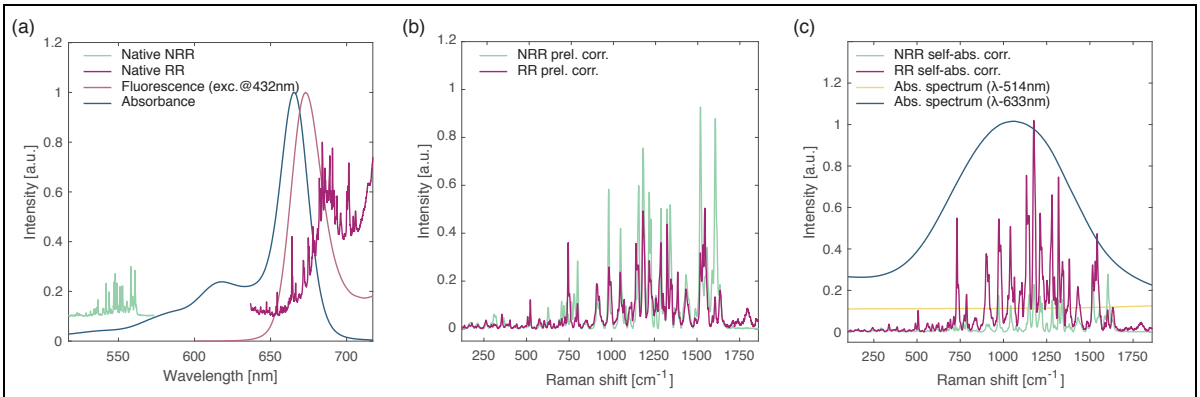

Fig. 4. Different steps in the correction process of RR (purple, exc. 633 nm) and NRR (light green, exc. 514 nm) Raman spectra. The same color code is maintained among the panels. (a) Native RR and NRR spectra. The spectra are reported in absolute wavelength. Absorption (blue) and fluorescence emission (pink) spectra of Chl*a* solutions are also shown as a reference. (b) Raman spectra preliminarily corrected for fluorescence background and instrumental factors (intensity of the exciting laser beam, integration time of the detector, wavelength sensitivity of the apparatus and dependence of the diffuse light on $\nu_L \nu_S^3$). (c) Raman spectra furtherly corrected for self-absorption phenomena occurring in the two considered spectral regions. The self-absorption normalization profiles, obtained from the absorption spectrum of the Chla powders, are reported in blue for excitation at 633nm and yellow for excitation at 514 nm, respectively.

Second, since RR and NRR are acquired at different wavelengths and using different laser sources, further corrections for the different instrumental factors such as the intensity of the exciting laser beam, I_0, and for the different integration time of the detector are necessary. Moreover, the spectrum must be corrected for the different wavelength sensitivity of the whole apparatus by dividing the spectrum by an instrumental response function determined by recording the spectrum of a power-calibrated lamp. Division of the data by this function corrects for the wavelength-dependent sensitivity of the apparatus, including optics, monochromator, and detector. Also, the dependence of the diffuse light on $\nu_L \nu_S^3$, where ν_L is the frequency of the exciting laser and ν_S is the frequency of the Raman diffused light, must be taken into account.

The results of the preliminary processing of RR and NRR spectra including the corrections for fluorescence and instrumental factors are shown in Fig. 4(b).

Moreover, the intensity of Raman signals can be attenuated by the sample self-absorption. When a careful identification of the vibrational modes most strongly enhanced in resonance condition is needed, as it is the case here for the comparison with 2DES data, the correction for self-absorption becomes crucial. The correction for self-absorption can indeed profoundly change the relative intensities of different Raman bands, depending on their frequency. Fig. 4(c) shows the RR and NRR Raman spectra after the correction for self-absorption phenomenon in the two exciting conditions. The correction has been performed normalizing the spectra with respect to the absorption spectrum of powders of Chl*a* in the two different spectral regions (see blue and yellow traces in panel (c)).

As for the fluorescence correction, also in this case the RR spectrum is the most affected because of the resonant conditions. It is important to notice that the main qualitative result after these multiple steps of correction is a general intensity enhancement of the Raman modes in the range 900-1500 cm^{-1} with respect to lower or higher frequency modes. This

evidence suggests a significant involvement of these modes in the coupling with the electronic transition generating the Q_y bands.

4. Discussion

The general approach to compare Raman and 2DES response relies on a qualitative frequency comparison. The beating patterns extracted at relevant 2D coordinates, suitably Fourier transformed, are compared with the Raman spectrum. Frequency components appearing in both spectra are then easily attributed to vibrational coherences. However, vibrational coherences are now recognized to be crucial for the correct description of the dynamical behavior of the materials, including dynamics of electronic coherences and transport processes. The increasing interest that these coherences are gaining calls for methodologies able of providing a comparison at a deeper level.

One of the points of major interest is the identification of the vibrational modes more strongly coupled with the electronic transitions since these are the modes that could be more actively involved in the modulation of relaxation and transport dynamics properties.

On the one hand, information on these modes can be directly extracted from the 2DES response (Fig. 3). Basing on the well-known DHO model, it is indeed possible to associate beatings at specific coordinates of the 2DES spectrum to a vibrational coherence in the ground ($g_1 g_0$) or in the excited state ($e_1 e_0$). From the comparison of beating frequencies at different coordinates, one can thus extract information on the modes more active in the excited state e. The possibility of examining both rephasing and non rephasing portions of the 2DES signal, suitably filtered by the laser bandwidth, provides a further advantage since it allows comparing oscillations of the signal at the *same* coordinates.

On the other hand, the investigation of $e_1 e_0$ coherences would strongly benefit by the support of Raman spectroscopy. Although the Raman technique can only capture ground state vibrations $g_1 g_0$, it is well known that, if the Raman spectrum is recorded in resonance with an electronic transition, only the modes more strongly coupled with that transition will be enhanced. In this sense, the identification of the Raman modes enhanced in resonant conditions could be directly related to the beating analysis in 2DES response.

It should be anyway recognized that a quantitative mode-by-mode comparison between Raman spectra and 2DES Fourier spectra is not particularly meaningful due to the undoubted lower precision of the 2D technique in determining the vibrational frequencies [51].

The difference in resolution lies in the intrinsically different nature of the techniques: the Raman spectroscopy is a steady state, frequency resolved technique; 2DES is an ultrafast time-resolved technique, where the frequency information is recalled through Fourier transform operations. Because of that, 2DES has the recognized advantage of making accessible simultaneously frequency and time information, identifying not only the frequency of the modes more strongly coupled with the electronic transition but also their dynamics and dephasing time. This could be crucial information to understand how the coupling with vibrational degrees of freedom affects the first steps of ultrafast relaxation dynamics [33,52]. However, as it has already been pointed out [39], the possibility of retaining information both in time and frequency domain can only be achieved at the cost of losing some resolution

along the frequency axis. And this is precisely why a conscious comparison with the Raman spectra, as proposed here, could be so crucial for the final interpretation.
Moreover, the quantitative description of the coupling between normal modes and the electronic transition would require the estimation of Huang-Rhys factors, not easily extracted from 2DES maps, unless with the support of quantum mechanical calculations [51].
Nevertheless, a qualitative comparison could be particularly useful to explain the different intensity distributions of the vibrational modes in rephasing and non rephasing datasets.
Fig. 5 compares Raman spectra with 2DES Fourier spectra. The light green and blue-green traces represent NRR and non rephasing Fourier spectra, both expected to provide information on ground state vibrations. Similarly, purple and red traces compare RR and rephasing Fourier spectra, which instead should preferentially underline modes more strongly coupled with the electronic transition.
Although a one-by-one correlation of the signals is not possible for the reasons discussed above, a first look at the spectra immediately reveals several points of similarity.
Both RR and rephasing Fourier spectra are dominated by vibrational modes in the 1000-1300 cm^{-1} range, whose intensity is drastically enhanced in resonance conditions, meaning that they are the most coupled with Q_y transition. In agreement with previous literature, the emergence of a mode at about 750 cm^{-1} is also witnessed, already identified as an important mode coupled with the Q bands transitions [24,30,31]. Other modes below 1000 cm^{-1} and above 1300 cm^{-1}, although identifiable, have an amplitude almost negligible.
NRR and non rephasing Fourier spectra show instead a higher number of relevant modes with comparable intensity, in particular in the regions 300:400 cm^{-1}, 600 cm^{-1}, 680:820 cm^{-1}, 890:1360 cm^{-1}, and 1480:1660 cm^{-1}.
These correlations suggest that, indeed, rephasing and non rephasing 2D signals, under suitable conditions, can be directly related to resonant and non resonant Raman spectra for the identification of the vibrational modes coupled with a specific electronic transition. Once demonstrated the validity of this approach, we can think of extending this procedure varying the excitation conditions both in Raman and in the 2DES analysis, to verify if similar or different modes couple with different electronic transitions. This information could be particularly relevant not so much for chlorophyll as an isolated chromophore in solution, but rather in complex systems bearing chlorophyll as energy or charge transfer unit. The possibility of verifying which vibrational modes are more strongly coupled with the different electronic transitions involved in the transport process would indeed actively advance our knowledge of the role of nuclei motion in such processes.

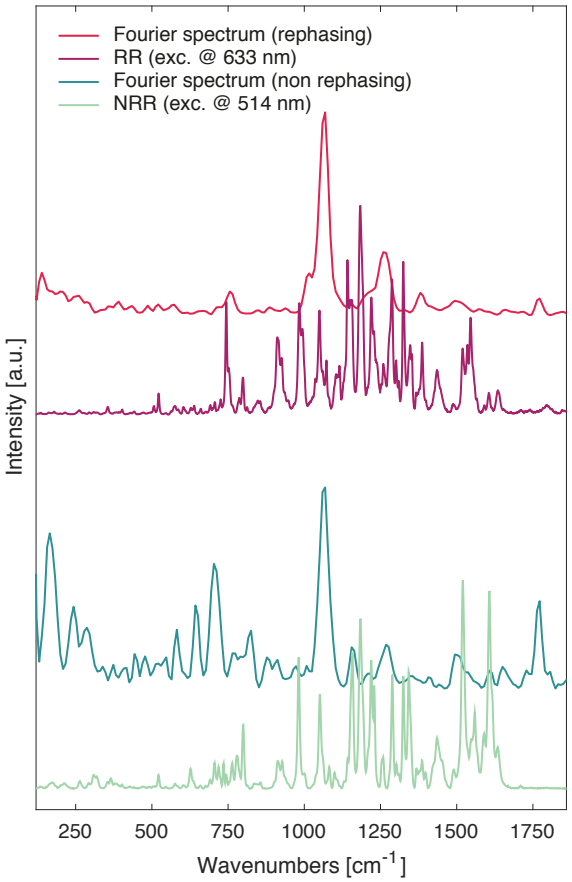

Fig. 5. Comparison between Raman and 2DES Fourier spectra. Upper section: RR spectrum (purple) and rephasing Fourier spectrum (red). Lower section: NRR spectrum (light green) and non rephasing Fourier spectrum (blue-green). The Fourier spectra show the square of the absolute value of the Fourier transform of the complex 2DES data over the population time [30,31].

5. Conclusions

When a beating frequency is detected in 2DES datasets of systems is not always trivial to tell whether its nature is vibrational or electronic, especially when dealing with multichromophoric systems. Raman spectra are undoubtedly an essential resource for the analysis of 2DES data and more and more often they are invoked to support the interpretation of 2DES response.

The standard practice in the comparison Raman/2DES is to simply look for frequencies present in both signals. Indeed, when a particular frequency is present both in the Raman and in the 2DES spectra, it can be reasonably attributed to a vibrational mode.

Here we have demonstrated that more details and information can be extracted from a deeper analysis of the spectra, provided that particular experimental conditions and suitable normalization procedure are fulfilled.

In particular, we demonstrated that the Fourier spectra, obtained from the analysis of the signals beating in rephasing and non rephasing conditions at specific coordinates of 2DES maps, can be directly compared with resonant and non resonant Raman spectra. Vibrational

modes more strongly coupled with the resonant transition can thus be clearly identified. We found that, to achieve a meaningful comparison, it is crucial to correct RR and NRR spectra for the self-absorption of the sample.
The advantages of this approach were illustrated using Chl*a* chromophore as a case study. 2DES and Raman spectroscopy agreed on identifying a manifold of vibrational modes in the region 1000-1300 cm^{-1} most strongly coupled with the resonant Q_y transition.

Competing financial interests

The authors declare no competing financial interests.

Acknowledgement

This work is supported by the FP7 ERC Starting Grant QUENTRHEL (278560) and by MIUR PRIN (Prot. 2015XBZ5YA).

References

[1] Collini E. Spectroscopic signatures of quantum-coherent energy transfer. Chem Soc Rev 2013;42:4932. doi:10.1039/c3cs35444j.
[2] Brańczyk AM, Turner DB, Scholes GD. Crossing disciplines - A view on two-dimensional optical spectroscopy. Ann Phys 2014;526:31–49. doi:10.1002/andp.201300153.
[3] Engel GS, Calhoun TR, Read EL, Ahn T-K, Mančal T, Cheng Y-C, et al. Evidence for wavelike energy transfer through quantum coherence in photosynthetic systems. Nature 2007;446:782–6. doi:10.1038/nature05678.
[4] Lee H, Cheng Y-C, Fleming GR. Coherence dynamics in photosynthesis: protein protection of excitonic coherence. Science 2007;316:1462–5. doi:10.1126/science.1142188.
[5] Collini E, Scholes GD. Coherent intrachain energy migration in a conjugated polymer at room temperature. Science 2009;323:369–73. doi:10.1126/science.1164016.
[6] Chin AW, Prior J, Rosenbach R, Caycedo-Soler F, Huelga SF, Plenio MB. The role of non-equilibrium vibrational structures in electronic coherence and recoherence in pigment–protein complexes. Nat Phys 2013;9:113–8. doi:10.1038/nphys2515.
[7] Scholes GD, Fleming GR, Chen LX, Aspuru-Guzik A, Buchleitner A, Coker DF, et al. Using coherence to enhance function in chemical and biophysical systems. Nature 2017;543:647–56. doi:10.1038/nature21425.
[8] Turner DB. Energy transfer: Resonance is the key for coherence. Nat Chem 2017;9:196–7. doi:10.1038/nchem.2742.
[9] Tiwari V, Peters WK, Jonas DM. Electronic resonance with anticorrelated pigment vibrations drives photosynthetic energy transfer outside the adiabatic framework. Proc Natl Acad Sci U S A 2013;110:1203–8. doi:10.1073/pnas.1211157110.

[10] Christensson N, Kauffmann HF, Pullerits T, Mančal T. Origin of long-lived coherences in light-harvesting complexes. J Phys Chem B 2012;116:7449–54. doi:10.1021/jp304649c.
[11] Fragnito HL, Bigot JY, Becker PC, Shank C V. Evolution of the vibronic absorption spectrum in a molecule following impulsive excitation with a 6 fs optical pulse. Chem Phys Lett 1989;160:101–4. doi:10.1016/0009-2614(89)87564-5.
[12] Vos MH, Rappaport F, Lambry J-C, Breton J, Martin J-L. Visualization of coherent nuclear motion in a membrane protein by femtosecond spectroscopy. Nature 1993;363:320–5. doi:10.1038/363320a0.
[13] Chachisvilis M, Pullerits T, Jones MR, Hunter CN, Chachisvilis ' M, Pullerits T, et al. Vibrational dynamics in the light-harvesting complexes of the photosynthetic bacterium Rhodobacter sphaeroides. Chem Phys Lett 1994;224:345–51. doi:10.1016/0009-2614(94)00560-5.
[14] Chachisvilis M, Fidder H, Pullerits Tõn, Sundström V. Coherent nuclear motions in light-harvesting pigments and dye molecules, probed by ultrafast spectroscopy. J Raman Spectrosc 1995;26:513–22. doi:10.1002/jrs.1250260706.
[15] Christensson N, Dietzek B, Yartsev A, Pullerits T. Electronic photon echo spectroscopy and vibrations. Vib Spectrosc 2010;53:2–5. doi:10.1016/j.vibspec.2010.01.009.
[16] Grimm B, Porra RJ, Rüdiger W, Scheer H. Chlorophylls and Bacteriochlorophylls (Advances in Photosynthesis and Respiration). Dordrecht: Springer; 2006.
[17] Björn LO, Papageorgiou GC, Blankenship RE, Govindjee. A viewpoint: Why chlorophyll a? Photosynth Res 2009;99:85–98. doi:10.1007/s11120-008-9395-x.
[18] Kobayashi M, Akutsu S, Fujinuma D. Physicochemical properties of chlorophylls in oxygenic photosynthesis - Succession of co-factors from anoxygenic to oxygenic photosynthesis. Rijeka: InTech; 2013.
[19] Gouterman M. Spectra of porphyrins. J Mol Spectrosc 1961;6:138–63. doi:10.1016/0022-2852(61)90236-3.
[20] Gouterman M, Wagnière GH, Snyder LC. Spectra of porphyrins: Part II. Four orbital model. J Mol Spectrosc 1963;11:108–27. doi:10.1016/0022-2852(63)90011-0.
[21] Asano M, Koningstein JA. Probing of chlorophyll a with a pulsed tunable laser: Monomer and dimer excited state lifetimes and their time resolved fluorescence spectra. Chem Phys 1981;57:1–10. doi:10.1016/0301-0104(81)80015-8.
[22] Binnie NE, Haley L V., Mattioli TA, Thibodeau DL, Wang W, Koningstein JA. Determination of in vitro chlorophyll a using wavelength-selective and time-resolved fluorescence. J Phys Chem 1986;90:4938–41. doi:10.1021/j100412a014.
[23] Thomas LL, Kim J-H, Cotton TM. Comparative Study of Resonance Raman and Surface-Enhanced Resonance Raman Chlorophyll a Spectra Using Soret and Red Excitation. J Am Chem SOC J Am Chem Soc I Sverdlov, L M; Kovner, M A; Krainov E P Vib Spectra Polyat Mol 1990;112:9378–86. doi:10.1021/ja00181a046.
[24] Zhou C, Diers JR, Bocian DF. Qy-excitation resonance Raman spectra of chlorophyll a and related complexes. Normal mode characteristics of the low-frequency vibrations. J Phys Chem B 1997;101:9635–44. doi:10.1021/jp971965g.
[25] Martinsson P, Oksanen J a. ., Hilgendorff M, Hynninen PH, Sundström V, Åkesson E. Dynamics of ground and excited state chlorophylla molecules in pyridine solution probed by femtosecond transient absorption spectroscopy. Chem Phys Lett

1999;309:386–94. doi:10.1016/S0009-2614(99)00710-1.
[26] De Boni L, Correa DS, Pavinatto FJ, Dos Santos DS, Mendoņa CR. Excited state absorption spectrum of chlorophyll a obtained with white-light continuum. J Chem Phys 2007;126. doi:10.1063/1.2722755.
[27] Rätsep M, Linnanto J, Freiberg A. Mirror symmetry and vibrational structure in optical spectra of chlorophyll a. J Chem Phys 2009;130:1–11. doi:10.1063/1.3125183.
[28] Telfer A, Pascal AA, Bordes L, Barber J, Robert B. Fluorescence line narrowing studies on isolated chlorophyll molecules. J Phys Chem B 2010;114:2255–60. doi:10.1021/jp907537a.
[29] Bricker WP, Shenai PM, Ghosh A, Liu Z, Enriquez MGM, Lambrev PH, et al. Non-radiative relaxation of photoexcited chlorophylls: theoretical and experimental study. Sci Rep 2015;5:13625. doi:10.1038/srep13625.
[30] Senlik SS, Policht VR, Ogilvie JP. Two-color nonlinear spectroscopy for the rapid acquisition of coherent dynamics. J Phys Chem Lett 2015;6:2413–20. doi:10.1021/acs.jpclett.5b00861.
[31] Moca R, Meech SR, Heisler IA. Two-dimensional electronic spectroscopy of chlorophyll a: solvent dependent spectral evolution. J Phys Chem B 2015;119:8623–30. doi:10.1021/acs.jpcb.5b04339.
[32] Wells KL, Zhang Z, Rouxel JR, Tan H. Measuring the spectral diffusion of chlorophyll a using two-dimensional electronic spectroscopy. J Phys Chem B 2013;117:2294–9. doi:10.1021/jp310154y.
[33] Meneghin E, Leonardo C, Volpato A, Bolzonello L, Collini E. Mechanistic insight into internal conversion process within Q-bands of chlorophyll a. Sci Rep 2017;7:11389. doi:10.1038/s41598-017-11621-2.
[34] Butkus V, Zigmantas D, Valkunas L, Abramavicius D. Vibrational vs. electronic coherences in 2D spectrum of molecular systems. Chem Phys Lett 2012;545:40–3. doi:10.1016/j.cplett.2012.07.014.
[35] Turner DB, Dinshaw R, Lee K-K, Belsley MS, Wilk KE, Curmi PMG, et al. Quantitative investigations of quantum coherence for a light-harvesting protein at conditions simulating photosynthesis. Phys Chem Chem Phys 2012;14:4857–74. doi:10.1039/c2cp23670b.
[36] Bolzonello L, Volpato A, Meneghin E, Collini E. Versatile setup for high-quality rephasing, non-rephasing, and double quantum 2D electronic spectroscopy. J Opt Soc Am B 2017;34:1223. doi:10.1364/JOSAB.34.001223.
[37] Kane DJ, Trebino R. Characterization of arbitrary femtosecond pulses using frequency-resolved optical gating. IEEE J Quant Electron 1993;29:571–9. doi:10.1109/3.199311.
[38] Volpato A, Bolzonello L, Meneghin E, Collini E. Global analysis of coherence and population dynamics in 2D electronic spectroscopy. Opt Express 2016;24:24773–85. doi:10.1364/OE.24.024773.
[39] Volpato A, Collini E. Time-frequency methods for coherent spectroscopy. Opt Express 2015;23:20040–50. doi:10.1364/OE.23.020040.
[40] Reimers JR, Cai Z-L, Kobayashi R, Rätsep M, Freiberg A, Krausz E. Assignment of the Q-bands of the chlorophylls: coherence loss via Qx - Qy mixing. Sci Rep 2013;3:2761. doi:10.1038/srep02761.

[41] Cipolloni M, Fresch B, Occhiuto I, Rukin P, Komarova KG, Cecconello A, et al. Coherent electronic and nuclear dynamics in a rhodamine heterodimer–DNA supramolecular complex. Phys Chem Chem Phys 2017;19:23043–51. doi:10.1039/C7CP01334E.
[42] Halpin A, Johnson PJM, Tempelaar R, Murphy RS, Knoester J, Jansen TLC, et al. Two-dimensional spectroscopy of a molecular dimer unveils the effects of vibronic coupling on exciton coherences. Nat Chem 2014;6:196–201. doi:10.1038/nchem.1834.
[43] Kjellberg P, Brüggemann B, Pullerits T. Two-dimensional electronic spectroscopy of an excitonically coupled dimer. Phys Rev B - Condens Matter Mater Phys 2006;74:1–9. doi:10.1103/PhysRevB.74.024303.
[44] Romero E, Augulis R, Novoderezhkin VI, Ferretti M, Thieme J, Zigmantas D, et al. Quantum coherence in photosynthesis for efficient solar-energy conversion. Nat Phys 2014;10:676–82. doi:10.1038/nphys3017.
[45] Fuller FD, Pan J, Gelzinis A, Butkus V, Senlik SS, Wilcox DE, et al. Vibronic coherence in oxygenic photosynthesis. Nat Chem 2014;6:706–11. doi:10.1038/nchem.2005.
[46] May V, Kühn O. Charge and energy rransfer dynamics in molecular systems. Weinheim, Germany: Wiley-VCH Verlag GmbH; 2003. doi:10.1002/9783527602575.
[47] Mukamel S. Principles of nonlinear optical spectroscopy. Oxford: Oxford University; 1995.
[48] Spencer AP, Hutson WO, Harel E. Quantum coherence selective 2D Raman–2D electronic spectroscopy. Nat Commun 2017;8:14732. doi:10.1038/ncomms14732.
[49] Peterman EJG, Wenk S-O, Pullerits T, Pålsson L-O, van Grondelle R, Dekker JP, et al. Fluorescence and absorption spectroscopy of the weakly fluorescent chlorophyll a in cytochrome b6f of synechocystis PCC6803. Biophys J 1998;75:389–98. doi:10.1016/S0006-3495(98)77523-X.
[50] Lee D, Albrecht AC. A unified view of Raman, resonance Raman, and fluorescence spectroscopy (and their analogues in two-photon absorption). In: Clark RJH, Hester RE, editors. Adv. infrared Raman Spectrosc. vol. 12, Chichester: Wiley; 1985, p. 179–213.
[51] Dean JC, Scholes GD. Coherence spectroscopy in the condensed phase: insights into molecular structure, environment, and interactions. Acc Chem Res 2017;50:2746–55. doi:10.1021/acs.accounts.7b00369.
[52] Bolzonello L, Polo A, Volpato A, Meneghin E, Cordaro M, Trapani M, et al. Two-dimensional electronic spectroscopy reveals dynamics and mechanisms of solvent-driven inertial relaxation in polar BODIPY dyes. J Phys Chem Lett 2018:1079–85. doi:10.1021/acs.jpclett.7b03393.

Appendix A. Supplementary data

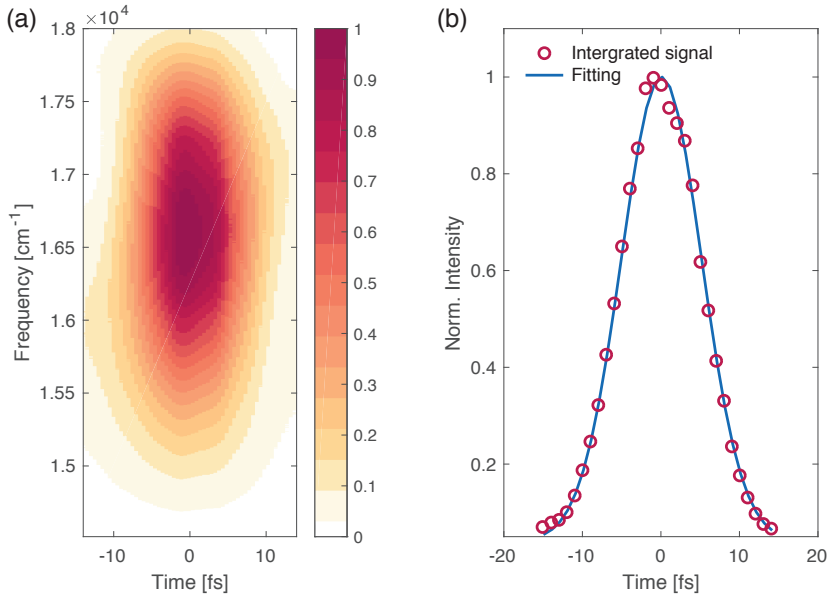

Fig. S1. (a) FROG measurement performed at the sample position in a 1mm cuvette filled with solvent. (b) Frequency integrated signal (circles) fitted with a Gauss function (blue line). The pulse duration is estimated to be 9 fs. The intensities in both panels are normalized to 1 on their maxima.

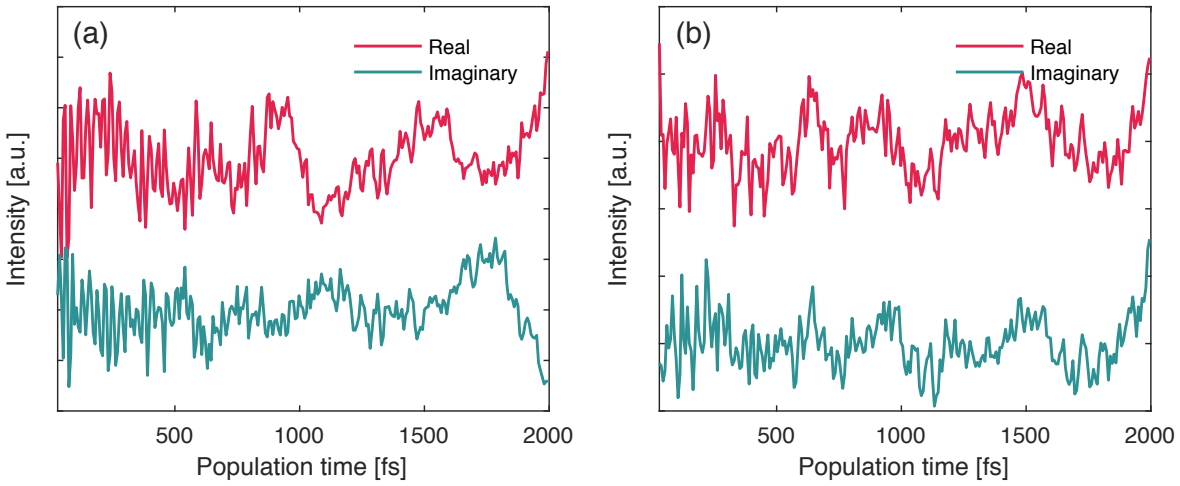

Fig. S2. Oscillating part of the rephasing (a) and non rephasing (b) signals at coordinates $(\varepsilon, \varepsilon + \Omega)$. Both real (red) and imaginary (green) part of the 2DES signal are reported.

Table S1. Frequency of vibrational coherences revealed in 2DES measurements and vibrational Raman modes. Ground (excited) state vibrations, determined from non rephasing (rephasing) experiment, are compared with NRR (RR) signals. As reference, we also report the results of fluorescence line narrowing (FLN), pump probe and T-RACS experiments from the literature, where ground and excited states vibrations have been explicitly distinguished. Numbers in bold point out the main signals. Values in cm^{-1}.

Ground state					**Excited state**				
2D non reph	**NRR**	**FLN (S_0)[a]**	**Pump probe[b]**	**T-RACS[c]**	**2D reph**	**RR**	**FLN (S_1)[a]**	**Pump probe[b]**	**T-RACS[c]**
--	--	--	--	--	140	--	--	--	--
165	173	--	--	--	--	179	--	--	--
--	212	--	--	--	210	216	--	214	--
240	264	--	--	--	**260**	**263**	**262**	**259**	--
285	294	--	--	--	285	295			
	309					310		300	
	319					320			
	355	--	--	--	**355**	**355**	**345**	**346**	--
370	365					378	371		
	378				390	385	388		
	402					393			
						403		407	
440	--	--	--	--	435	430		--	--
						442			
480	--	--	--	--	--	485	468	--	--
--	506	--	--	--	--	506	--	--	--
520	522	--	519	--	520	522	519	--	--
550							535		
580	576	574	--	--	**570**	**576**	**570**	**565**	--
584						587			
--	603	--	--	--	--	604	601	--	--
--	627	--	621	--	--	628	--	--	--
	638					639			
640	659	--	667	--	670	660	--	667	--
	676					693			
	692					700			
	705				710	707			
710	719					725			
	735								
	744	**744**	**744***	**743**		**744**	**740**	**744***	**738**
				754	**755**	752			748
765	764	--		--	--	787	--	--	--
825	779					799			
	800		799						
--	--	--	--	--	851	847	--	--	--
						855			
875	913	--	915*	--	--	911	--	915*	--
910	927					926			
970	982	985	982*	--	1015	984	984	982*	--
	1000		1043			994		1043	
1070	1051	--	--	--	**1070**	**1049**	**1106**	**1084**	--
	1082					1073			
	1100		1124*			1115		1124*	
1155	1157	1146	--	--	--	1141	1133	--	--
						1151			
						1156			
	1184	1189	--	--		1184	1170	1175	--
1215	1220				1215	1220			
	1229					1228			
--	1259	--	1251*	--	**1260**	**1259**	**1245**	**1251***	--

1270	1289	--	--	--	--	1288	--	--	--
						1302			
--	1325	1331	--	--	--	1325	--	--	--
--	1342	--	--		--	1347	1347		--
				1353*		1353		1353*	
--	1387	--	--	--	1380	1387	--	--	--
--	1435	--	1415	--	--	1435	--	--	--
1495	1490	--	--	--	1495	1487	--	1460	--
	1520		1516*			1520	1514	1516*	
--	--				--	1535	1534		
--	--				--	1546			
--	1547	1540			--	--			
	1559	1556							
1610	1590		1582		--	1606		1613	
	1608								
1650	1635		1648		--	1636			
1770	--				1770	1795		1770	

(a) Vibrational frequencies of Chl*a* in Cytochrome b6f from line narrowed emission measures taken from Ref. [Biophys J 1998;75:389–98]. Only modes labelled as 'strong' have been included.
(b) [Biophys J 2011;101:995–1003]. The modes labeled with * have not been assigned by the authors and therefore are reported here in both columns.
(c) [J Phys Chem Lett 2015;6:2413–20].